Nuclear Inst. and Methods in Physics Research, A 931 (2019) 172–180

Contents lists available at ScienceDirect

Nuclear Inst. and Methods in Physics Research, A

journal homepage: www.elsevier.com/locate/nima

3D thermal-fluid coupled analysis for 81.25 MHz RFQ accelerator ☆

Bo Zhao [a,b], Tieming Zhu [b], Fengfeng Wang [b], Xiaofeng Jin [b], Chenxing Li [b], Wei Ma [b], Shuping Chen [a,*], Xinlong Zhu [b], Bin Zhang [b]

[a] Lanzhou University of Technology, Lanzhou 730000, Gansu China
[b] Institute of Modern Physics, Chinese Academy of Science, Lanzhou 730000, China

ARTICLE INFO

Keywords:
RFQ
Thermal-fluid coupled analysis
Frequency
Temperature

ABSTRACT

The thermal stability of the radio frequency quadrupole (RFQ) is an important concern during commissioning. The cooling water takes away the power dissipated on the RFQ internal surface to maintain the thermal stability and limit the structural deformation. In this paper, the thermal-fluid coupled analysis of the RFQ is described and 3D temperature distribution of the RFQ cavity structure is given. The method of adjusting the water temperature is determined through analysis. The heat transfer coefficient for the cooling channels and the outlet water temperature about the water cooling system are obtained. A comparison of the results in simulation and experiment is presented. The cooling system can meet the requirements of RFQ operating.

1. Introduction

A four-vane CW Radio Frequency Quadrupole (RFQ) Accelerator has been designed as a key equipment for the Low Energy highly-charged ion Accelerator Facility (LEAF) project at the Institute of Modern Physics, Chinese Academy of Sciences. The RFQ will accelerate ion species from proton to uranium from 14 keV/u up to 0.5 MeV/u [1].

The RF power dissipation on the internal surface of the cavity can heat the cavity and cause RFQ deformation. The cooling system is utilized to maintain the thermal stability and limit the structural deformation. It is important to analyze the cooling process of the RFQ, which is used to simulate the temperature rise, the deformation and the frequency shift [2–11]. The whole 3D analysis considering the fluid flow can be studied to obtain more intuitive and complete analysis results.

In this paper, the detailed 3D coupling analysis of the RFQ is performed including electromagnetic (EM), thermal-fluid coupled analysis and structural simulation by using ANSYS workbench [12]. Fig. 1 shows the procedure of the analysis. The actual shape of the U-cooling channel is considered to simulate the true flow of the fluid in the channel. Fig. 2 shows the U-cooling channel of the cavity.

2. Geometric parameters of RFQ cavity

As shown in Fig. 3, the RFQ accelerator made of oxygen-free copper is equally divided into six segments, each with a length of 994.82 mm. Each segment comprises four machined vanes and four machined walls. The eight machined parts are welded together to form one segment. No coupling plate is used between the segments [1]. A metal gasket is used to insure good RF contact between adjacent segments. The RFQ is equipped with a total of 48 tuners. Fig. 3 is the structure layout of the cavity with tuners, which are uniformly distributed along the beam direction. The RF power is delivered by two couplers, which are located at the wall of the second and third segments of the cavity. π-mode stabilizing loops (PISLs) are used for mode separation to avoid the adjacent dipole mode mixing [8]. The main parameters of RFQ are summarized in Table 1 [8,9].

3. Coupled analysis procedure

3.1. The radio frequency analysis

The RF simulations were performed with Micro Wave Studios (MWS) [8] and High Frequency Structure Simulator (HFSS). The power loss of the full length cavity is calculated through MWS. The distribution of power losses is simulated by HFSS in ANSYS [12], and is applied to the internal surfaces of the RFQ cavity. Fig. 4 shows the 3D model in HFSS. A comparison of the results calculated by MWS and HFSS codes is shown in Table 2.

3.2. Thermal-fluid coupled analysis

The simulated total power loss on the whole cavity is 56.56 kW [8]; the real total losses are expected to be higher up to 20% [11]. It is provided that the heat load of 11.3 kW on each segment is all

☆ Work supported by the NSFC (contract No. 11427904)
* Corresponding author.
E-mail address: chensp@lut.cn (S. Chen).

https://doi.org/10.1016/j.nima.2019.03.032
Received 3 January 2019; Received in revised form 22 February 2019; Accepted 12 March 2019
Available online 15 March 2019

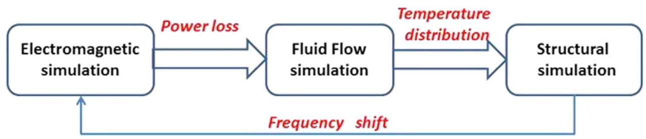

Fig. 1. Analysis procedure with HFSS and ANSYS.

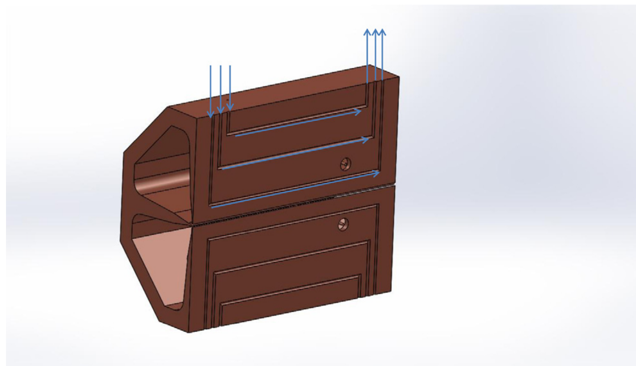

Fig. 2. U-cooling channel of the cavity.

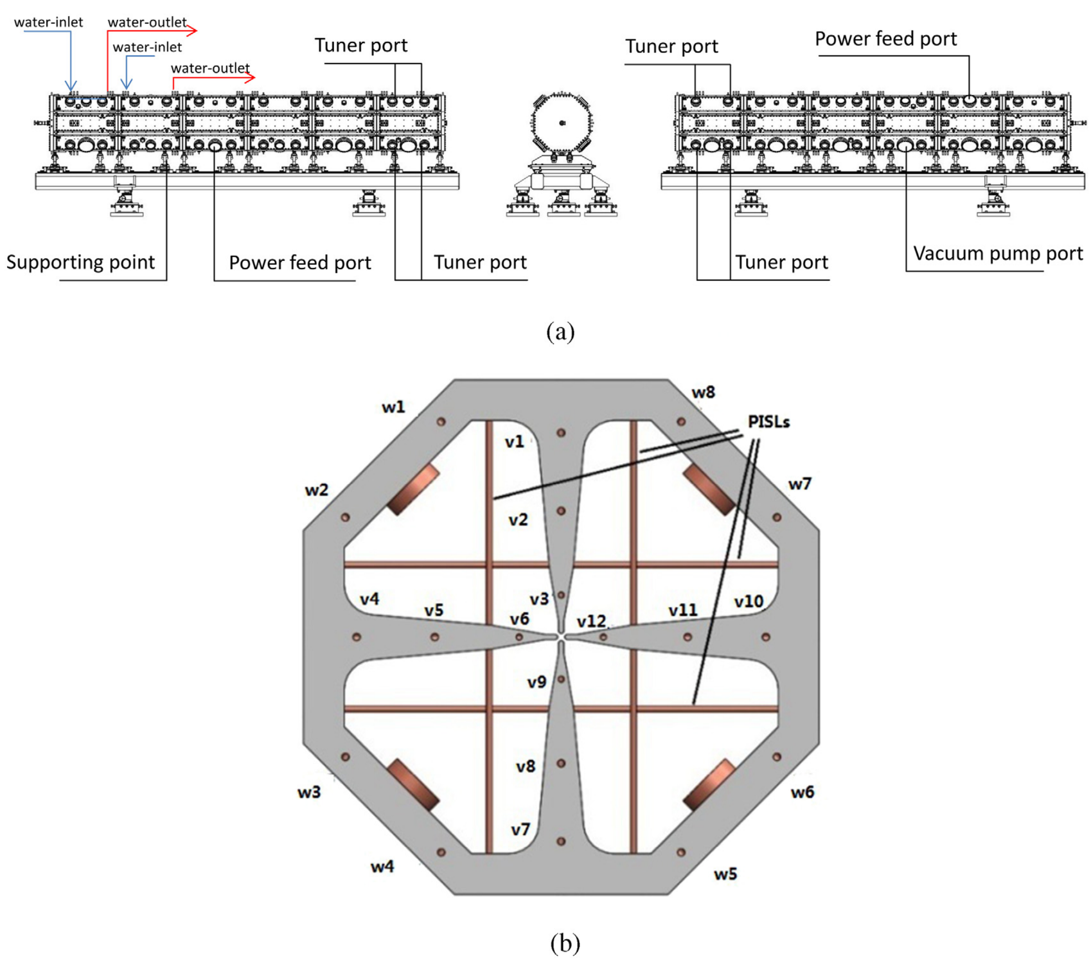

Fig. 3. Structure of RFQ cavity (a) and the flow distribution of RFQ cavity (b).

removed by cooling water. Two methods can be used to obtain the heat-transfer coefficients of the cooling-water channels, one is to perform the thermal-fluid coupled analysis for direct simulation, and the other is to use the empirical formulas to calculate the values. ANSYS Fluent is a computer program for modeling fluid flow, heat transfer in complex geometries. Based on FLUENT, the first approach is adopted. The results of simulation are also checked with the calculated values from the empirical formulas.

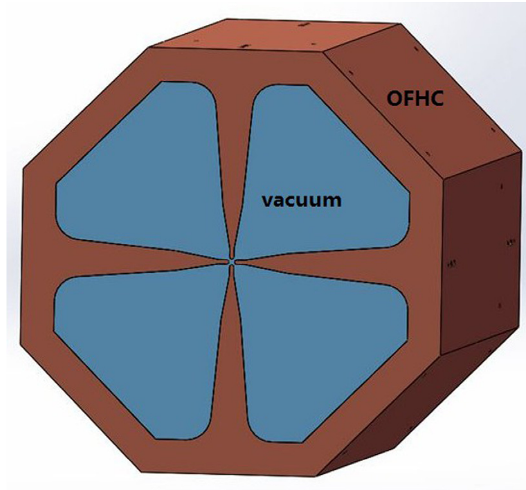

Fig. 4. RFQ model of RF simulation in HFSS.

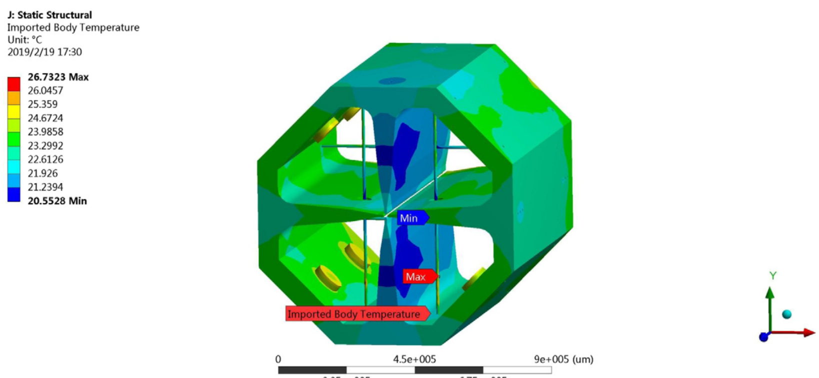

Fig. 5. Temperature distribution of the cavity.

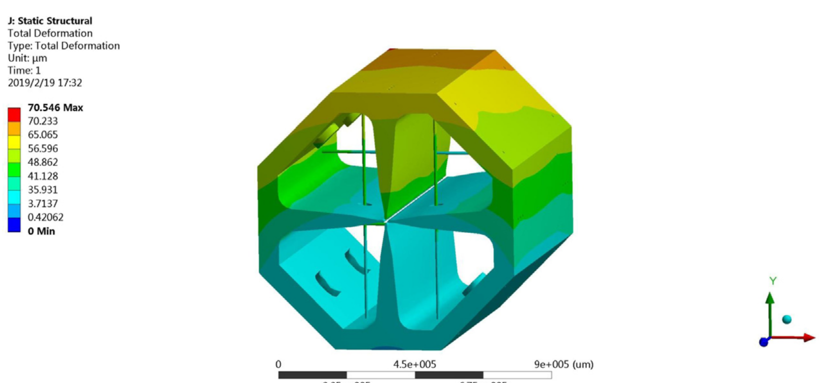

Fig. 6. Displacement distribution.

The cooling water temperature and ambient temperature are set to 20 °C. The convective heat transfer coefficient between the outer wall and air is 10 W/m^2*K. The parameters of cooling water for the different cooling channels are listed in Table 3. The Reynolds numbers are higher than 10,000, which indicate the flows are turbulent in all channels. A pressure-based solver is used to deal with this problem of incompressible flow, and the k-epsilon turbulent model is used to compute the flow process in the channels. The temperature distribution of the cavity at steady state analysis is shown in Fig. 5, which is between 20 °C and 27 °C.

3.3. Mechanical analysis and frequency shift calculation

The cavity temperature distribution obtained from thermal-fluid coupled analysis is imported to the structural analysis. Meanwhile, the fixed boundary condition based on the support and the vacuum pressure condition are applied in the structural analysis. A pressure of

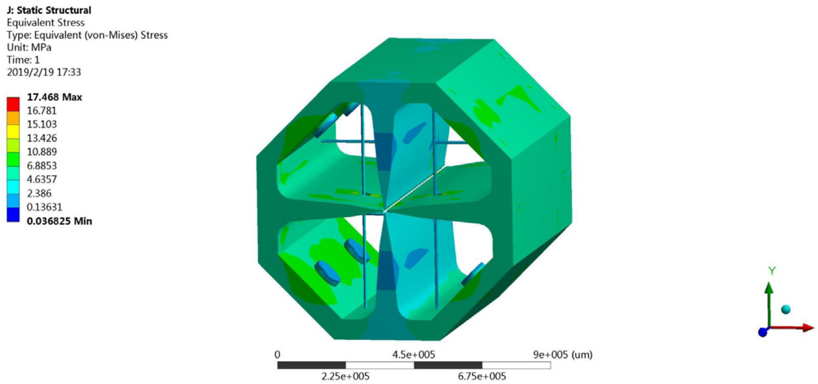

Fig. 7. Stress distribution.

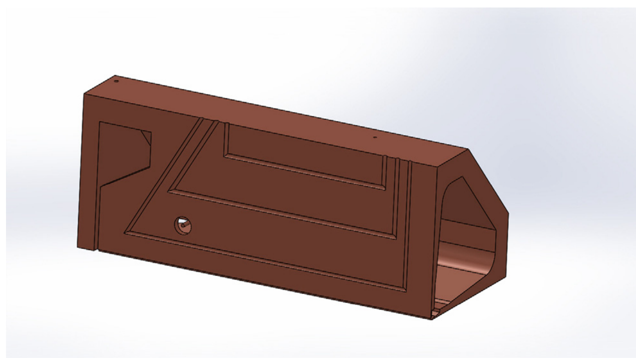

Fig. 8. A quarter of the RFQ model at the end regions of vanes.

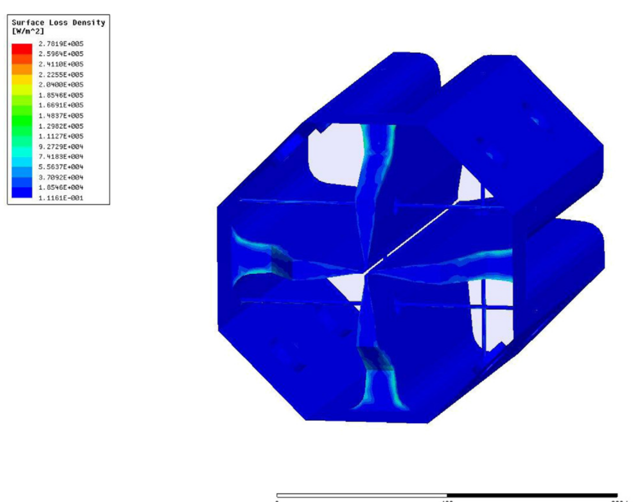

Fig. 9. Distribution of the power loss on the vane cutbacks.

10,133 Pa is applied on the outer walls and fixed support is applied on supporting point (see Fig. 3). The displacement distribution and the stress distribution are given in Figs. 6 and 7. The maximum displacement of the cavity is located at external surface. The yield strength of oxygen free copper after annealing is 60–70 MPa [1]. As shown in Fig. 7, the maximum stress is calculated to be 17.5 MPa, which is below the yield strength of OFHC. The displacement of the cavity can cause the frequency shift. According to the result of displacement, the frequency shift at full power is 10.5 kHz compared to the initial frequency simulated with HFSS.

3.4. Coupled analysis of the end regions

Considering cutbacks at the end regions of RFQ vanes (entrance/exit), the Multi-physics analysis of the end regions must be considered. A quarter of the RFQ model at the end regions of vanes is shown in Fig. 8. Fig. 9 shows the distribution of the power loss on the vane

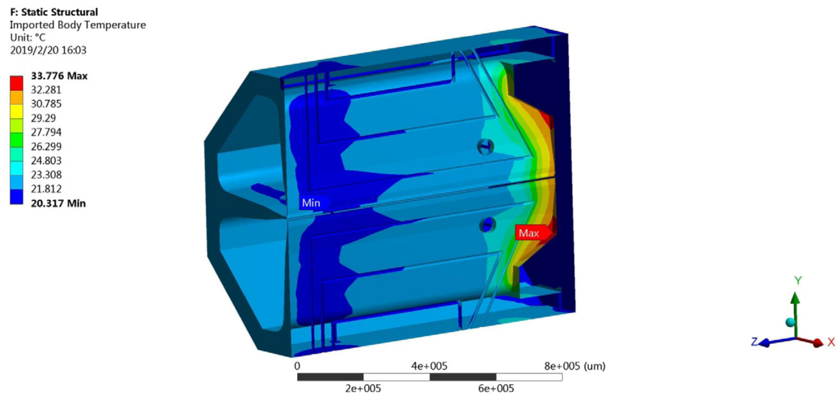

Fig. 10. Temperature distribution of cutbacks.

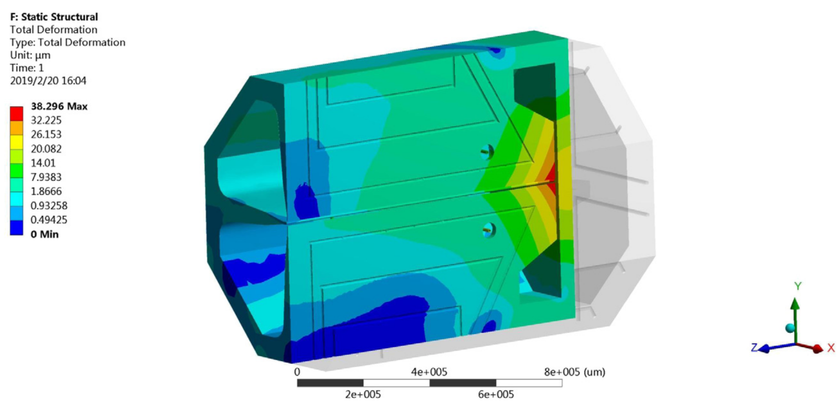

Fig. 11. Deformation distribution of cutbacks.

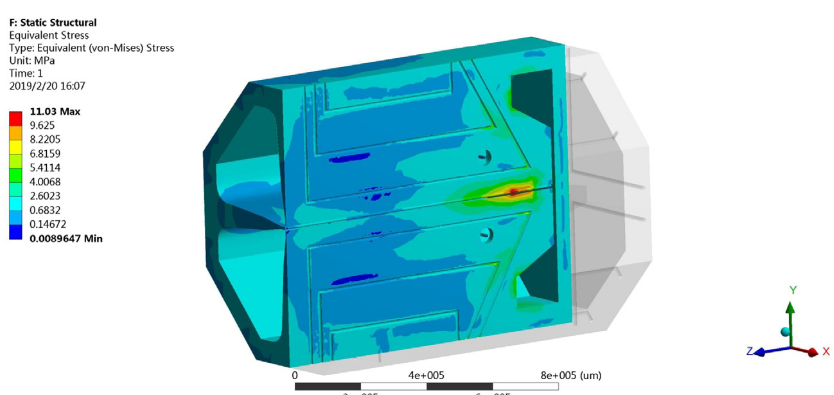

Fig. 12. Stress distribution of cutbacks.

cutbacks. The temperature distribution is given in Fig. 10. Figs. 11 and 12 show the distributions of the deformation and the stress at the end region. The maximum temperature and the deformation of the end region are 33.8 °C and 38 μm, respectively. The cavity deformation will affect RFQ performance, such as the accelerating and focusing functions. Permanent inelastic deformation of the cavity should be avoided during long time operation. These deformation results meet the design requirement.

4. Analysis of the water cooling process

4.1. Theoretical calculation and verification

The heat transfer coefficient between the cooling water and the wall of cooling channel can be calculated as following equation [13]

$$h = Nu * k/D$$

where k is the thermal conductivity of the water, D is channel diameter, Nu is the Nusselt number,

$$Nu = 0.023 Re^{0.8} Pr^{0.4}$$

Re represents the Reynolds number, and Pr is Prandtl number,

$$Re = \frac{\rho v D}{\mu}$$

$$Pr = \frac{c_p \mu}{k}$$

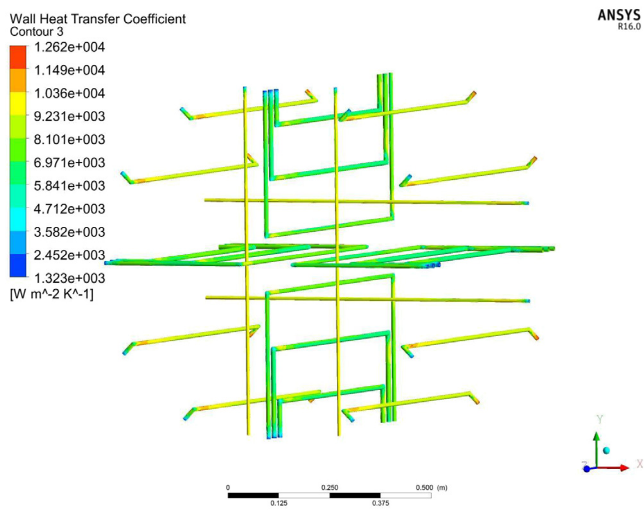

Fig. 13. Heat transfer coefficient on the walls of channels.

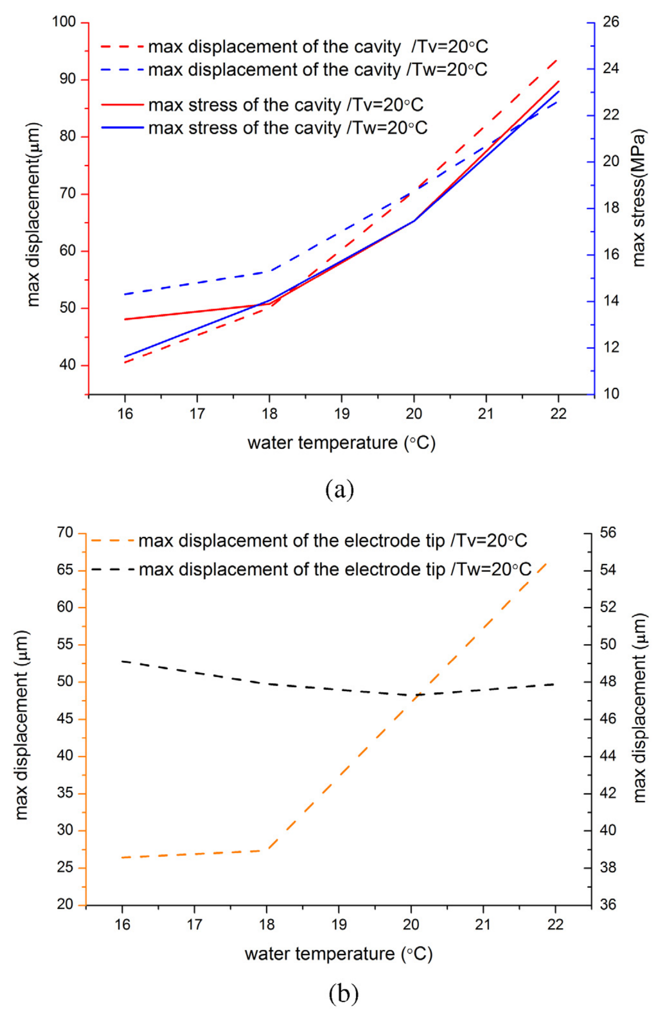

Fig. 14. Relationships both the maximum displacement and stress of the cavity (a) and the maximum displacement of the electrode tip (b) with the water temperature.

Here υ, ρ, μ correspond to fluid flow velocity, fluid density and viscosity coefficient respectively.

Fig. 13 shows the heat transfer coefficient on the channel walls based on the simulation. The comparison of results between simulation and calculation are listed in Table 4. The direct results of thermal-fluid coupled simulation are slightly larger than the calculation results of empirical formula. This coupling simulation method can obtain the fluid parameters and observe the cooling effect intuitively.

4.2. The effect of water temperature on frequency

The responses of maximum displacement and stress of the cavity, when altering the cooling water temperature in the vane channels (T_v) and wall channels (T_w) are plotted in Fig. 14(a), and the maximum deformation of the electrode tips caused by the change of the cooling water temperature shown in Fig. 14(b). The maximum displacement and stress are changed by the increase or decrease of the water temperature.

As shown in Fig. 15, through the linear fitting, the tuning coefficients of T_v and T_w are calculated as −15.565 kHz/°C and 13.685 kHz/°C, respectively. The temperature of the wall at which there is no frequency shift is 19.22 °C when fixed T_v at 20 °C, and the temperature of the vane at which there is no frequency shift is 20.655 °C when fixed T_w at 20 °C. It is suggested that T_v should be higher than T_w during tuning the cavity.

5. Experimental processes

5.1. Water cooling system

Fig. 16 shows the complete water cooling system of the RFQ cavity. The full cavity consists of 72 vane cooling channels and 24 wall cooling channels (the wall channels in series per wall) and 12 pairs of π-mode stabilizing loops (PISLs) cooling channels. The cooling system provides two separate chillers for the RFQ cavity, one for the walls and PISLs, and one for the vanes. Since the vane is more sensitive to water temperature, the electric diverting valve is set in the vane loop to mix warm water with cold water to improve the accuracy of water temperature regulation. A part of warm water from the main water return pipe flows back into the main water supply pipe. In the control system, the electric actuator of electrical valve is adjusted to control the mass flow based on the resonance frequency error signal provided by the Low Level RF (LLRF) control system. In addition, there are the water

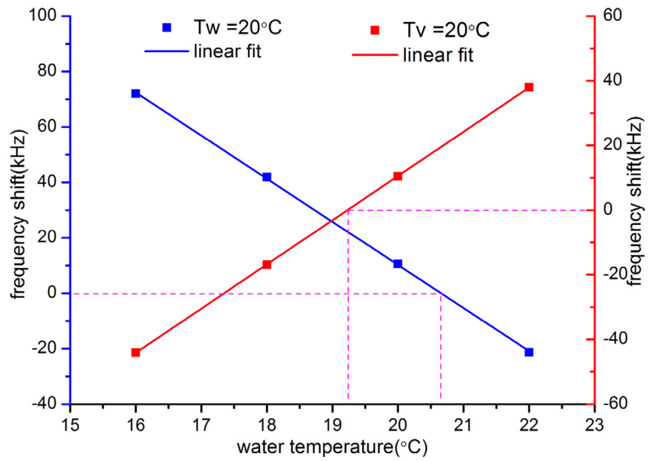

Fig. 15. Effect of the cooling water temperature on the frequency shift of the cavity.

manometers, thermometers and flowmeters in the system. An overview of the RFQ cavity with water cooling devices is shown in Fig. 17. The water temperature is monitored in the experiment to check the validity of the thermal-fluid coupled analysis.

5.2. Experimental results and comparison with simulation

The frequency and field distribution of the full cavity were measured. The quadrupole and dipole perturbative components of the field are suppressed to 0.8% and 1.5%, respectively [1]. The measured Q value is 16,230 and the frequency is 81.254 MHz [1].

The experiment is carried out under the CW He^+ ion beam with the power loss of 24 kW and the cavity vacuum of 10^{-5} Pa. The inlet temperatures of wall cooling water and vane cooling water are adjusted as 20 °C and 20.5 °C, respectively, to maintain the cavity frequency. Through the water temperature group obtained, it is verified that the T_v should be higher than T_w. According to the structure symmetry, the experimental data of vane channels in vertical and lateral directions are selected. The consistency of the results between experiment and simulation is listed in Table 5. Fig. 18 shows the real-time monitoring chart. The five lines at the top of the chart (from top) represent the outlet water temperatures of V-L1, V-L3, V-L2, W-UR, PISLs, respectively. The brown line at the bottom shows the frequency. It is clearly indicated that the experimental results can prove the validity of the simulation. The correctness of the model and method are confirmed.

6. Conclusion and future plan

Three dimensional integrated thermal-fluid coupled simulations are performed in order to calculate accurately heat exchange between cooling water and the cavity. The fluid flow and thermal characteristics are analyzed. Comparing with experimental results under the same conditions, the validity of the simulation model and method is proven. The analysis processes can also be used in other RF structures. Considering the cooling process changes with time, further studies will include the thermal-fluid coupled transient analysis.

Acknowledgments

The author would like to thank Mr. Yuhui Guo, Mr. Yuting Liu, Mr. Yang Yao, Mr. Chuanfei Hu, Mr. Hongyi Ma , Mr. Huan Jia,for their efforts on experiments. This work is supported by National Natural Science Foundation of China (11427904).

Table 1
Main parameters of the cavity.

Parameters	Value
Frequency (MHz)	81.25
Input energy (keV/u)	14
Output energy (MeV/u)	0.5
Inter-vane voltage (kV)	70
Total length of the vane (mm)	5946.92
Mean aperture (mm)	5.805
Vane tip radius	4.354
Kilpatrick factor	1.55
Peak current (emA)	2
Transmission efficiency (%)	97.2
Number of vane cooling channels	72
Number of wall cooling channels	48
Power loss (kW)	56.56

Table 2
RF simulation results comparison.

Parameters	MWS [8]	HFSS
Frequency (MHz)	81.246	81.1075
Q factor	17,963	18,448

Table 3
The parameters of cooling water for the different cooling channels.

Part	Velocity (m/s)	Temperature (°C)	Diameter (mm)
w1~w8	2.0	20	10
v (3/6/9/12)	1.5	20	10
The other v	1.5	20	12
PISL	2.0	20	8

Table 4
Comparisons between theoretical and simulated values of heat transfer coefficient.

Part	Heat transfer coefficient	
	Theoretical values (W/m^2*K)	Simulated values (W/m^2*K)
w1~w8	8253.01	9062.52
v (3/6/9/12)	6556.34	7154.39
v (1/4/7/10)	6321.56	6970.52
v (2/5/8/11)	6321.56	7006.06
PISL	8629.68	9228.37

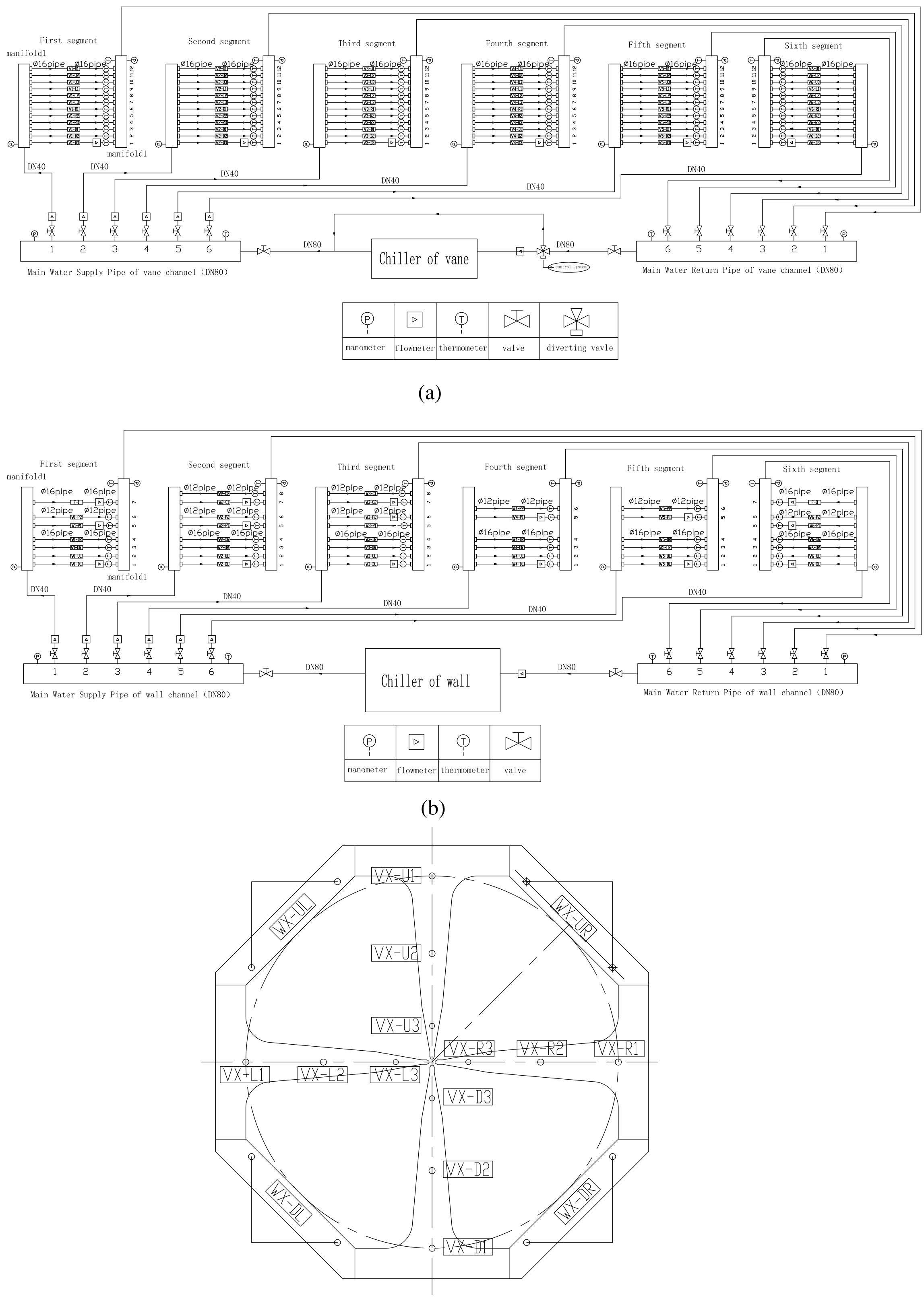

Fig. 16. Water cooling scheme and monitoring layout, (a) is for the vane and (b) is for the wall and (c) is the monitoring marker.

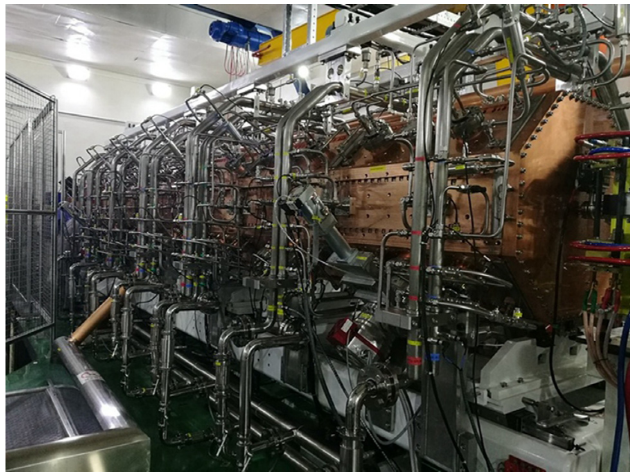

Fig. 17. View of the RFQ cavity with water cooling devices.

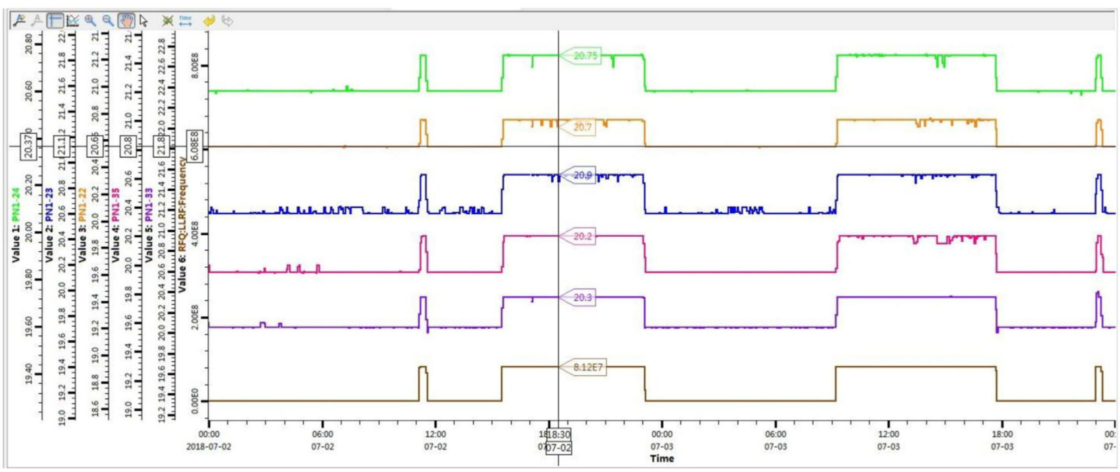

Fig. 18. Real-time monitoring chart. (For interpretation of the references to color in this figure legend, the reader is referred to the web version of this article.)

Table 5
Comparisons between experimental and simulated values of outlet water temperatures.

Part	Outlet water temperatures	
	Experimental values (°C)	Simulated values (°C)
PISL	20.3	20.421
W-UR	20.2	20.384
V-L1	20.75	20.764
V-L2	20.79	20.878
V-L3	20.9	21.015
V-U1	20.7	20.663
V-U2	20.7	20.656
V-U3	20.9–21.0	20.771

References

[1] W. Ma, Study On the Low Energy High Current High Charge State RFQ (Dissertation of Master Degree), University of Chinese Academy of Sciences, 2018.
[2] Z.H. Peng, et al., Thermal analysis of high current proton RFQ cavity, At. Energy Sci. Technol. 39 (2) (2005) 160–163.
[3] F. Scantamburlo, et al., 3D thermo mechanical study on IFMIF-EVEDA RFQ, in: Proceedings of LINAC2010, Tsukuba, Japan, 2010, pp. 539–541.
[4] Z.L. Zhang, et al., Design of a four-vane RFQ for CHINA ADS project, in: Proceedings of LINAC2012, Tel-Aviv, Israel, 2012, pp. 942–944.
[5] R. Tiede, et al., A coupled RFQ-IH-DTL cavity for Franz: A challenge for RF technology and beam dynamics, in: Proceedings of HB2016, Malmö, Sweden, 2016, pp. 404–408.
[6] J. Wang, et al., Frequency tuning with RFQ temperature in China ADS injector II, Chin. Phys. C 40 (3) (2016) 037003-1-037003-5.
[7] J. Wang, et al., Multi-physics analysis of the RFQ for injector II scheme of C-ADS driver linac, Chin. Phys. C 38 (10) (2014) 107005-1-107005-5.
[8] W. Ma, et al., Design of an 81.25 MHz continuous-wave radio-frequency quadrupole accelerator for low energy accelerator facility, Nucl. Instrum. Methods Phys. Res. A 847 (2017) 130–135.
[9] W. Ma, et al., Three-dimensional multi-physics analysis and commissioning frequency tuning strategy of a radio-frequency quadrupole accelerator, Nucl. Instrum. Methods Phys. Res. A 866 (2017) 190–195.
[10] S.C. Joshi, et al., 3D thermal-fluid coupled analysis for 350 MHZ RFQ for INDIAN SNS PROGRAMME, in: Proceedings of APAC2004, Gyeongju, Korea, 2004, pp. 314–316.
[11] G. Romanov, et al., Project X RFQ EM design, in: Proceedings of IPAC2012, New Orleans, Louisiana, 2012, pp. 3883–3885.
[12] ANSYS, http://www.ansys.com.
[13] S.M. Yang, W.Q. Tao, Heat Transfer, Higher Education Press, Beijing, 2006.